

OPTIMIZATION AND VERIFICATION OF DOUBLE LAYER BEAM SHAPING ASSEMBLY (DLBSA) FOR EPITHERMAL NEUTRON GENERATION

Bilalodin*, Aris Haryadi, Kartika Sari, Wihantoro

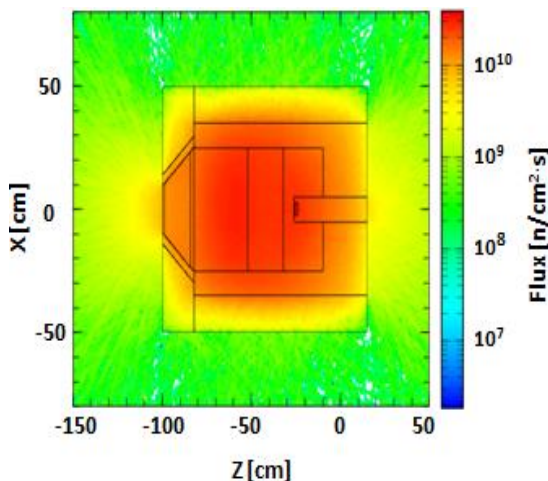
Department of Physics, Faculty of Mathematics and Natural Science, Jenderal Soedirman University, Indonesia

Article history

Received
29 November 2021
Received in revised form
23 March 2022
Accepted
31 March 2022
Published Online
20 June 2022

* Corresponding author:
bilalodin@unsoed.ac.id

Graphical abstract



Abstract

The designs of Beam Shaping Assembly (BSA) for moderating fast neutron into epithermal neutron have been conducted. Some BSA models that are previously developed are still having problems in generating epithermal neutron. Instead, we propose designs of double layer beam shaping assembly (DLBSA) to produce epithermal neutron. Optimization of the Double Layer Beam Shaping Assembly (DLBSA) design was carried out using the genetic algorithm (GA) method using MCNPX and verified using the Particle and Heavy Ion Transport code System (PHITS). The optimization resulted in four configurations up to the 21st generation capable of producing epithermal neutron beams that comply with the IAEA standards. The best four configurations are obtained by combining: (1) Al with one of the CaF_2 , BiF_3 or PbF_2 materials as moderator, (2) Pb with Pb, Ni, or Bi as a reflector, (3) Ni with FeC, or C as collimator, (4) (FeC + LiF) as fast neutron filter, Cd or B_4C as thermal neutron filter. Verification of the four optimum configurations of the DLBSA model using PHITS code shows that the epithermal neutron beam produced by DLBSA has met the IAEA standards.

Keywords: DLBSA optimization, verification, epithermal neutron, MCNPX, PHITS, BNCT

© 2022 Penerbit UTM Press. All rights reserved

1.0 INTRODUCTION

Boron Neutron Capture Therapy (BNCT) is a promising cancer therapy method, considering its possibility to kill cancer cells selectively by using neutron irradiated in-cell boron compound. The key success for therapies using the BNCT method is determined by two factors, namely accumulated boron compound in cancer cells and availability of adequate neutron sources [1, 2].

Current adequate neutron sources derived from nuclear reactors are very expensive and it is almost impossible to build nuclear reactor in hospitals. Therefore, neutron sources from accelerators are developed [3, 4]. A model of accelerator that is

currently being developed and is suitable for laboratory and hospital purposes is the cyclotron [5].

The neutrons produced by a cyclotron come from the interactions of protons with a target material. However, fast neutrons resulting from the interactions remain to be processed by moderating systems, such as the beam shaping assembly (BSA), to yield neutrons having range of energy in the level of epithermal neutrons 0.5 ~ 10 keV and low contaminants [6, 7]. The quality and quantity of the neutron beams to be utilized as a neutron source for BNCT must comply with the standards of IAEA TECDOC 1223 [8].

Some designs of BSA based on 30 MeV cyclotrons are continually developed. Three models are

developed for processing high energy neutron beams that result from reactions of 30 MeV protons with a beryllium target. The earliest model of BSA was introduced by Tanaka *et al.*, 2011 [9]. Their BSA model uses Pb material as neutron multiplier, and Al and CaF₂ as moderator. The moderator material is circumscribed by a Pb reflector. LiF combined with polyethylene is used as a filter for thermal neutron and Pb as gamma shielding. This configuration is able to produce epithermal neutron flux, but is still accompanied by contaminants, making it non-compliant with the IAEA standard.

Hasimoto *et al.*, (2014) constructed second BSA model to process neutron beams that results from the interactions of protons with a beryllium target ranging from 20 MeV to 30 MeV [10]. Such configuration of BSA consists of moderator, reflector, collimator, and filter. MgF₂ material is used as moderator and Pb as reflector. The wall of the collimator is made of two layers, i.e. PE 50% mixed with LiF and Pb. Fe and LiF are used as a filter for fast and thermal neutrons and Bi as gamma shielding. This configuration can produce epithermal neutron flux, but yet it contains contaminants of fast neutrons and gamma ray.

The third model of BSA was introduced by Khorsidi (2017) [11]. This model is used to process neutron beams from the interactions of a target and protons with energy of 15 MeV to 30 MeV. The moderator used in this model is Pb and fluental. Fluental is a combination of three materials, namely 69 w% AlF₃, 30 w% Al and 1 w% LiF. Pb is arranged to circumscribe the beryllium target, while fluental is placed on the surface of Pb. The reflector is made of graphite, and the collimator is made from Bi material coated by Boron Carbide (B₄C). In order to reduce contaminants, a filter consisting of Fe, Li, and Bi is installed, in which Li as a filter for thermal neutron, Bi as a filter for gamma ray, and Fe as a second filter for fast neutron. The resulting epithermal neutron is significantly high, but the accompanying contaminants are still high too.

The three models of BSA have not been able to produce neutron beams that completely meet the IAEA standards. This is presumably due to the use of a single layer configuration, which uses one type of material. According to Rasouli and Masoudi, (2012) one of the disadvantages of using a single layer configuration is that it is less than optimal for moderating neutrons and reducing contaminants in BSA [12]. Therefore, single-layer construction is being abandoned and multi-layer configurations began to be developed. The multilayer configuration utilizes more than one material in composing the components of BSA. One of the multilayer configurations is double layer. The double layer configuration produces an alloy of two materials that have better properties than the properties of each of the constituent materials [13].

The three models are also designed using stepwise optimization. Staged optimization is carried out by selecting the type of material and followed by

varying the thickness of the material through simulation. The weakness of the stepwise method is that the combined optimization results of each BSA component (moderator, reflector, collimator and filter) do not always produce an optimal beam. This is because each BSA constituent material affects each other in producing a radiation beam. According to Kasesaz *et al.*, (2014) BSA system actually belong to highly complex systems because the components that make up BSA are independent variables that are difficult to control and influence each other [14].

Methods that can be used to optimize complex systems include artificial neural networks (ANN), colony algorithms, and genetic algorithms (GA) [15]. ANN is an optimization method that mimics the human nervous system. The Colony algorithm is based on colony behaviour of living creatures, while GA is based on natural genetic selection and inheritance. The use of the GA method is deemed more suitable as a BSA optimization method. The selection properties of GA can be used to select good BSA constituent materials. Meanwhile, genetic inheritance can be used in choosing a combination of materials that have been selected for combining into two materials that can produce the most optimal BSA output. The optimized BSA components are expected to produce high epithermal neutron beams and low contaminants according to IAEA standards. In this article, we will describe the results of the BSA design using a double layer configuration and its optimization using genetic algorithm (GA) optimization. The optimal configuration results are verified using a program based on the Monte Carlo Particle and Heavy Ion Transport code System (PHITS) so that the design and optimization results using the GA method is highly valid.

2.0 METHODOLOGY

2.1 Optimization

The BSA design uses a double layer configuration. The neutrons come from reactions of 30 MeV protons with a ⁹Be target. Double Layer Beam Shaping Assembly (DLBSA) has four main components, namely moderator, reflector, collimator and filter. Each component is formed from a combination of two materials. The moderator was chosen from a combination of aluminum (Al) material and eight other moderator materials, namely Al₂O₃, LiF, AlF₃, MgF₂, CaF₂, BiF₃, PbF₂ and C₂F₄. The reflector is selected from a combination of Pb material with bismuth (Bi), carbon iron (FeC), Nickel (Ni) and graphite (C) materials. Choosing the right combination of fast neutron filter and thermal neutron is done by combining FeC with Cd, Ti, Li, B₄C and ¹⁰B materials. The double layer configuration of BSA is shown in Figure 1.

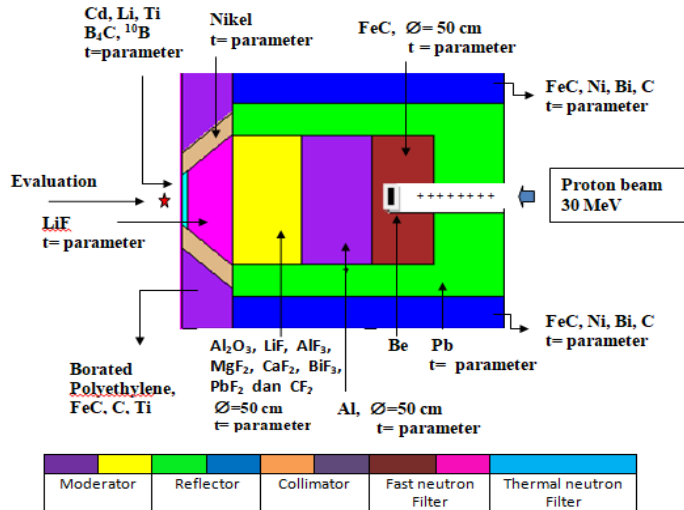


Figure 1 Configuration of double layer BSA

In order to obtain the optimal DLBSA configuration in generating neutron beams that comply with IAEA standards, a genetic algorithm (GA) optimization based on Monte Carlo N particle X (MCNPX) software is used. The implementation of GA in DLBSA optimization goes through the following steps: representing the chromosomes from DLBSA, calculating fitness function, performing selection, crossover, mutation, and convergence test. The representation of chromosomes in DLBSA is expressed in the form of an arrangement of DLBSA components, namely moderator, reflector, collimator and filter. The composition of the material and its thickness in each component is expressed as a gene. The first material that makes up the DLBSA component is called the superior gene and the second material is called non-superior. Superior genes are always involved in every process of forming a new generation. The materials used in the design and optimization of DLBSA and their relation to chromosomes and genes are shown in Table 1. Based on Table 1, each chromosome is made as an input program and run using the MCNPX program.

Table 1 Representation of chromosomes and genes of DLBSA

No	Moderator		Reflector				Collimator			Filter				Remark		
	m ₁	t ₁	m ₂	t ₂	m ₃	t ₃	m ₄	t ₄	m ₅	t ₅	m ₆	m ₇	t ₇		m ₈	t ₈
1	Al	10	Al ₂ O ₃	40	Pb	5	Ni	20	Ni	5	FeC	FeC	22	Cd	1	K1
2	Al	20	LiF	30	Pb	10	C	15	Ni	10	Ti	FeC	22	B ₄ C	2	K2
3	Al	30	AlF ₃	20	Pb	15	FeC	10	Ni	15	C	FeC	22	Li	3	K3
4	Al	40	MgF ₂	10	Pb	20	Bi	5	Ni	20	B-Poly	FeC	22	¹⁰ B	4	K4
5	Al	10	CaF ₂	40	Pb	5	Ni	20	Ni	5	FeC	FeC	22	Cd	1	K5
6	Al	20	BiF ₃	30	Pb	10	C	15	Ni	10	Ti	FeC	22	B ₄ C	2	K6
7	Al	30	PbF ₂	20	Pb	15	FeC	10	Ni	15	C	FeC	22	Li	3	K7
8	Al	40	CF ₂	10	Pb	20	Bi	5	Ni	20	B-Poly	FeC	22	¹⁰ B	4	K8

where t₁-t₈ = material thickness, m₁-m₈ = type of material, t and m are expressed as genes. K1-K8 are expressed as chromosomes

The output of each chromosome is calculated for its fitness value, which is stated in Equation 1.

$$F = (w_1 \Delta \phi_{epi} + w_2 \Delta R_{epi/th} + w_3 \Delta R_{epi/fast} + (w_4 \Delta D_f + w_5 \Delta D_\gamma) / 10^8) \tag{1}$$

where : w₁, w₂, w₃, w₄, and w₅ are weight = 1

$$\begin{aligned} \Delta \phi_{epi} &= (\phi_{epi} - 10^8) \\ \Delta R_{epi/th} &= (\phi_{epi} / \phi_{th} - 100) \\ \Delta R_{epi/fast} &= (\phi_{epi} / \phi_{fast} - 100) \\ \Delta D_f &= (D_f / \phi_{epi} - 10^{-13}) \\ \Delta D_\gamma &= (D_\gamma / \phi_{epi} - 10^{-13}) \end{aligned}$$

Weight factors w₁-w₅ are set uniformly =1 for their being equally significant in their contribution to generate chromosomes.

The fitness value of each chromosome was tested for its convergence. Convergence conditions occur when the value of the fitness function of the chromosomes tends to be constant [16]. If it is not satisfied, the selection step is continued. The selection process was carried out to determine the potential probabilities of the chromosomes in producing five beam parameters according to IAEA standards. The selection makes use of Equation 2 [17].

$$F_s = (F_i / \sum F_i) N \tag{2}$$

where F_s = selection function, F_i = the i-th fitness function, N = number of chromosomes/individual in a generation.

Chromosomes that have passed the selection are brought into crossovers and mutations to get a new generation. In this case, the material type or thickness of one of the selected chromosomes is exchanged with another chromosome. The crossover and mutation processes continue to progress in each stage until a convergent condition is reached [18]. Value of the fitness function, selection, crossover and mutation are carried out with the help of the Python program.

2.2 Simulation process of DLBSA optimization using Genetic Algorithm (GA)

The process of optimization simulation carried out from the 0-th generation chromosome is shown in Table 2. Input program for eight chromosomes in Table 2 is written in MCNPX 2.7 program [19]. The MCNPX program was run using 10^6 particle history with a multiplier of 6.25×10^{15} n/s in *n p h* mode and F5 tally for the calculation of the thermal neutron beam, epithermal neutron, and fast neutron parameters. The calculation of gamma dose rate and fast neutron dose rate uses the DE and DF tally. Microscopic cross-section data for simulation use ENDF/B-VII and Visual Editor to create geometric visualizations from MCNPX inputs. For accuracy in data the simulation run with a statistical error of < 10 %. The design and optimization flowchart as well as the simulation of the DLBSA simultaneously using the AG method is shown in Figure 2.

2.2 Verification of the neutron beam of DLBSA in optimal configuration

The design of BSA that has been successfully created using GA optimization (optimal configuration) is then verified using another design in the same form using the Particle and Heavy Ion Transport code System (PHITS) program [20].

The PHITS program belongs to Monte Carlo-based programs. As such, it can be used as a benchmark for other programs that are also based on Monte Carlo [21]). The verification of the neutron beam produced by DLBSA is carried out by calculating the neutron spectrum using Tally Track

The calculation of the fast neutron dose rate and gamma dose is used by Tally Track which is equipped with K_{fast} and K_{γ} conversion factors to convert.

3.0 RESULTS AND DISCUSSION

3.1 Design and Optimization of DLBSA using Genetic Algorithm (GA)

DLBSA is a system that processes fast neutrons into epithermal neutrons and functions to reduce contaminants. The system has four main components, namely moderator, reflector, collimator, and filter. Each component is formed from a combination of two materials. The use of two materials in each DLBSA component is intended to enhance the contribution of each material. The initial three-dimensional design of the DLBSA using MCNPX programming visualized in the Vised software is shown in Figure 3.

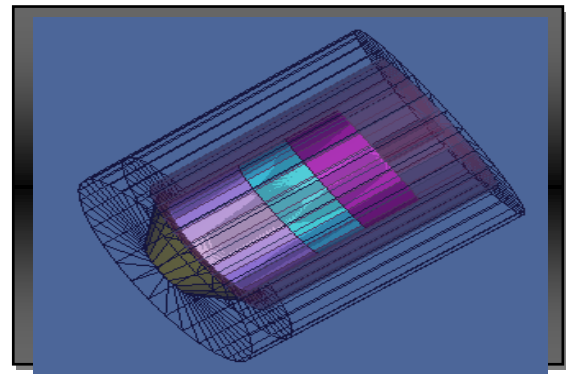


Figure 3 Three dimensional view of DLBSA

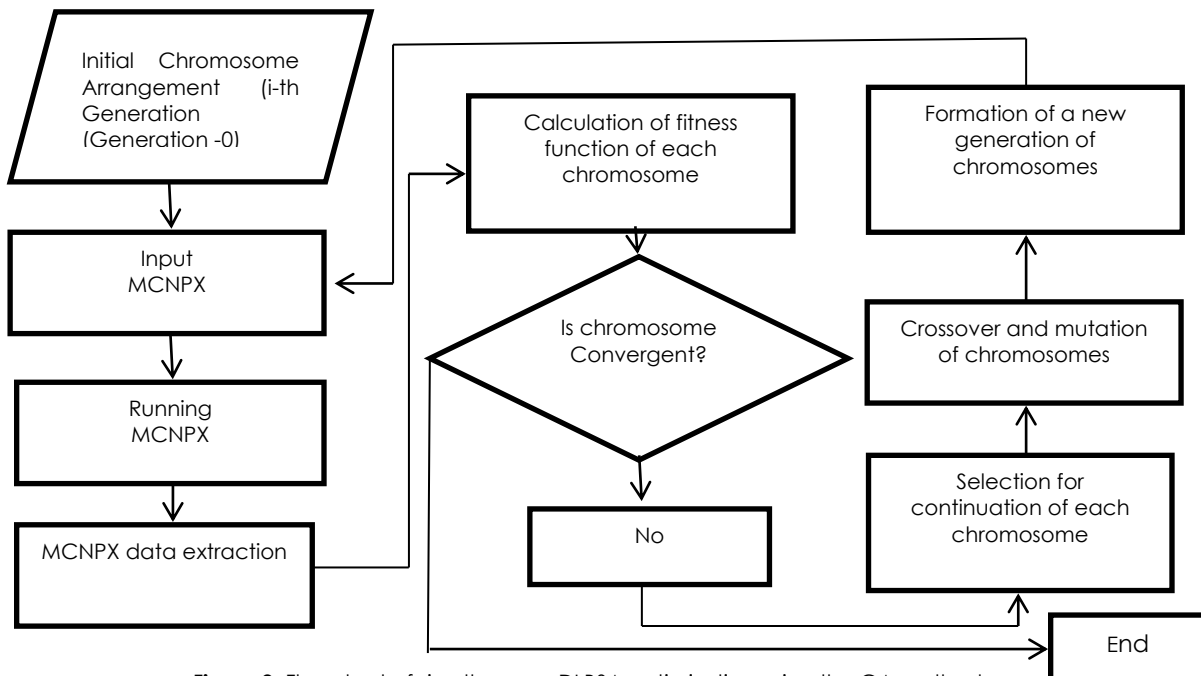


Figure 2 Flowchart of simultaneous DLBSA optimization using the GA method

Table 2 Comparison of the characteristics of the first generation radiation beam with the desired solution (IAEA standard)

No	K	$Q_{epi} \times 10^9$ (n/cm ² .s)	Q_{epi}/Q_{th}	Q_{epi}/Q_{fast}	D_{fas}/Q_{epi} $\times 10^{-13}$ (Gray.cm ²)	D_{γ}/Q_{epi} $\times 10^{-13}$ (Gray.cm ²)
1	K1	1.02	405	23	9.32	0.246
2	K2	0.15	122	3	5.48	0.486
3	K3	0.63	203	8	1.98	0.149
4	K4	0.13	71	4	1.71	0.148
5	K5	1.40	667	15	2.71	0.957
6	K6	0.36	50	5	1.75	0.116
7	K7	0.69	137	69	5.41	0.141
8	K8	0.13	43	2	1.34	0.141
	IAEA (2001)	≥ 1.0	>100	>20	< 2.0	< 2.0

Optimization of DLBSA using the GA method was carried to obtain the best composition and geometric configuration of the DLBSA. The DLBSA is expected to produce neutron radiation beam parameters that agree with IAEA standards. The results of the first generation optimization of DLBSA for 8 chromosomes are shown in Table 2. Some chromosomes produce radiation beams that still deviate from IAEA standards. Table 3 shows that the highest epithermal neutron flux is 1.4×10^9 n/cm².s and the lowest is 1.3×10^8 n/cm².s. The other four radiation beam parameters do not meet the IAEA criteria. It suggests that the epithermal neutron beam still contains many contaminants. Based on these data, the first generation DLBSA is not sufficient to be a source of BNCT therapy. The characteristics of the neutron beam produced by the first generation DLBSA are shown in Table 2.

Based on Table 2, the optimization of DLBSA in the first generation has not been able to produce a neutron beam that meet the IAEA standard. Therefore, further optimization is carried out by increasing generations to get a convergent fitness function (fixed value). Convergent conditions indicate the attainment of an optimal solution, suggesting that a configuration capable of producing a neutron beam agreeing with IAEA standards has been found.

Figure 4 shows the relationship between the increase in generation and the fitness function. It shows that the larger the generation, the higher the fitness value. The fitness value in the 18th to 21st generations tends to be constant. This shows that this generation has reached convergence [16]. This means that the optimum solution has been attained. This is an indication that there are several DLBSA configurations capable of producing neutron beams that accord with IAEA standards.

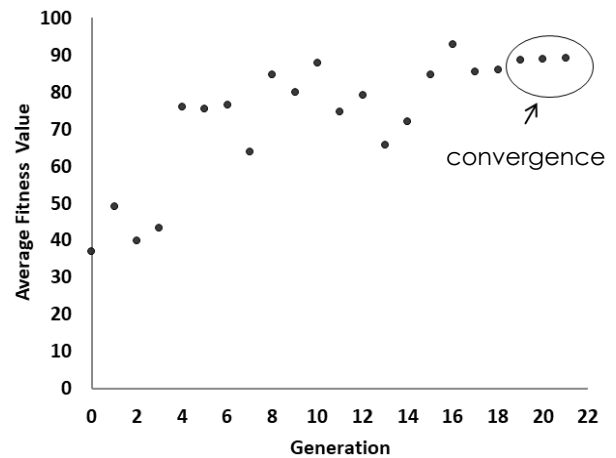


Figure 4 Relation of the increase in generation to the fitness value

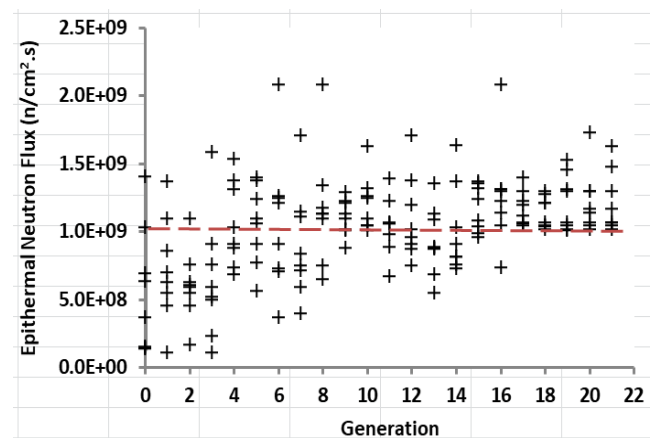


Figure 5 Effect of generation change on epithermal neutron flux

Figure 5 shows the effect of increasing generation on changes in epithermal neutron flux. A population whose chromosomes (individuals) produce a pareto optimal (optimal solution set) when the epithermal neutron flux is 1.0×10^9 n/cm².s [16]. The figure shows that increasing generations produces solutions that spread towards the optimal solution and all optimal

solutions are reached from the 18th generation to the 21st generation. The epithermal neutron flux as a solution in the 21st generation varies between $1.0\text{--}1.59 \times 10^9 \text{ n/cm}^2\cdot\text{s}$. The values of epithermal neutron flux have met the IAEA requirements. However, other requirements in the form of contaminants in the form of fast neutrons, thermal and gamma rays accompanying epithermal neutrons must be as low as possible

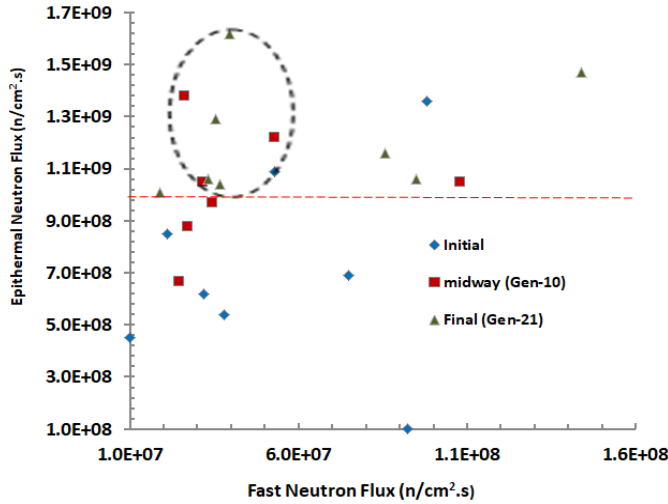


Figure 6 Value of fast neutron flux that accompany epithermal neutron flux in early, middle and late generation

In addition to fast neutron flux, thermal neutron flux accompanying the epithermal neutrons that directly emerge from the DLBSA must also be limited. The ratio between the epithermal neutron flux and the thermal neutron flux (Φ_{epi}/Φ_{ther}) should not be less than 100 [16]. Based on Figure 6 and 7, the value of the fast neutron flux that accompanies the epithermal neutron flux in the early, middle and late generations causes an increase in the epithermal neutron flux and a decrease in the thermal neutron flux. In the 21st generation some individuals have produced pareto (optimal completion set) 100 [16]. This shows that in the 21st generation some DLBSA configurations have met the IAEA requirements, namely the ratio between the epithermal neutron flux and the thermal neutron flux (Φ_{epi}/Φ_{ther}) ≥ 100 .

The effect of generation changes on the ratio between changes in the fast neutron dose rate and the gamma dose rate on the epithermal neutron flux are shown in Figures 8 and 9. The increase in generation produces a number of solutions in the form of a ratio of fast neutron dose value to the epithermal neutron flux that varies and the value tends to produce a solution towards the ratio of the fast neutron dose rate to the epithermal neutron flux (D_{fast}/Φ_{epi}) that approaches $2 \times 10^{-13} \text{ Gy}\cdot\text{cm}^2$. The optimization results pertaining to changes in the gamma dose rate to the epithermal neutron flux also resulted in a ratio of gamma dose rate and

epithermal neutron flux $< 2 \times 10^{-13} \text{ Gray}\cdot\text{cm}^2$. The optimization results in the final generation (Gen-21) have very low radiation contaminants (contaminants) in form of fast neutrons and gamma radiation. This shows that in the 21st generation several DLBSA configurations have met IAEA requirements, especially the ratio between changes in fast neutron dose rate and gamma dose rate to epithermal neutron flux $< 2 \times 10^{-13} \text{ Gray}/\text{cm}^2$.

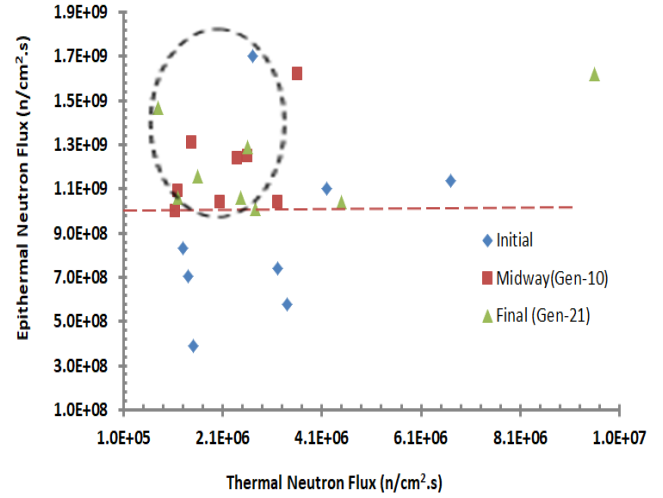


Figure 7 Value of thermal neutron flux accompanying epithermal neutron flux in early, middle and late generations

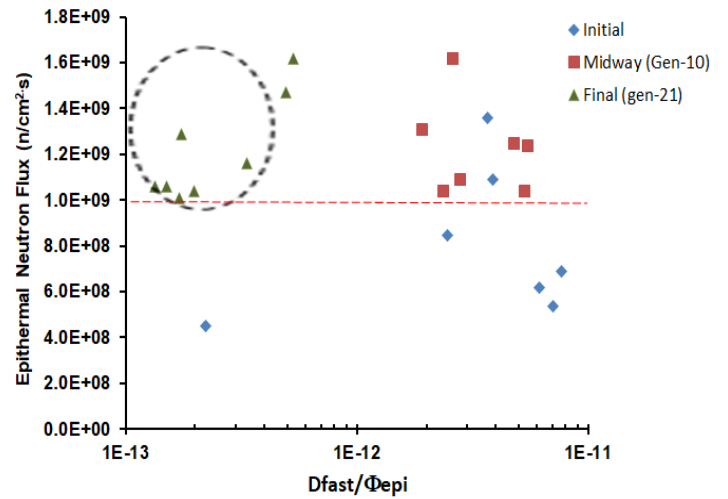


Figure 8 Effect of generation change on the ratio between fast neutron dose rate and epithermal neutron flux in early, middle and late generations

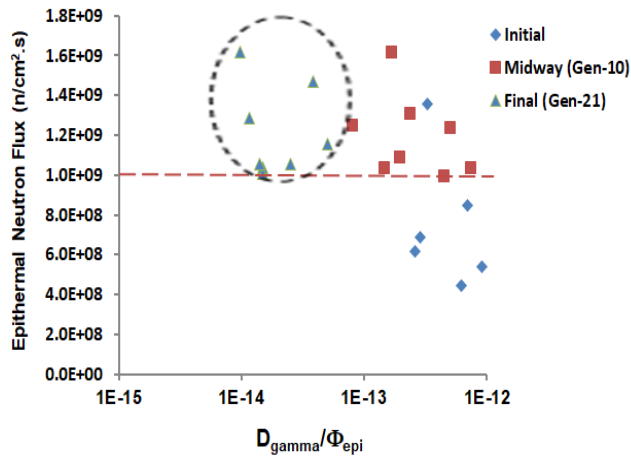


Figure 9 Effect of generation change on the ratio between gamma dose rate and epithermal neutron flux in early, middle and late generations

The optimization of the DLBSA configuration until the 21st generation resulted in four (4) configurations that reached the optimum condition. The value of radiation beam parameter from the DLBSA has met the IAEA standards. The parameter values of the 21st

generation radiation beam are shown in Table 3. The optimal configuration is obtained by combining the Al material with one of the PbF₂, BIF₃ or CaF₂ materials as a moderator. The best reflectors can be formed by combining Pb material with Ni, Pb or Bi materials. The best collimator is formed by combining Ni material with FeC and C materials. In order to reduce fast neutron contaminants, thermal and gamma it is highly recommended to use Fe, Cd and B₄C. The success of optimization using the GA method cannot be separated from the use of superior genes such as Al, Pb, Ni, FeC and Cd, which are always involved in every process of forming a new generation.

3.2 Verification of Neutron Beams Produced by DLBSA

Verification of outgoing neutron beams from DLBSA is conducted using the PHITS code. The PHITS code has simple procedures in using tally and excellent graphic display output [20]. The input of PHITS code uses 4 (four) best configurations from the optimization using the GA method shown in Table 4.

Table 3 Parameters of radiation beam resulting from optimization of DLBSA using the GA

No	21 st Generation Chromosome	Qepi x10 ⁹ (n/cm ² .s)	Qepi/Qth	Qepi/Qfast	Dfas/Qepi X 10 ⁻¹³ (Gray.cm ²)	Dy/Qepi X 10 ⁻¹³ (Gray.cm ²)
1	K1	1.47	1865	10	9.32	0.246
2	K2	1.16	725	14	5.48	0.486
3	K3	1.04	231	28	1.98	0.149
4	K4	1.01	367	53	1.71	0.148
5	K5	1.62	169	41	2.71	0.957
6	K6	1.29	496	36	1.75	0.116
7	K7	1.06	891	11	5.41	0.141
8	K8	1.06	431	32	1.34	0.141
	IAEA (2001)	≥1.0	>100	>20	< 2.0	< 2.0

Table 4 Configurations of double layer BSA that produce optimum radiation beam obtained from optimization of BSA using the GA method

K	Moderator				Reflector				Collimator			Filter			
	M ₁	t ₁	M ₂	t ₂	M ₁	t ₁	M ₂	t ₂	M ₁	t ₁	M ₂	M ₁	t ₁	M ₂	t ₂
K3	Al	32	PbF ₂	18	Pb	20	Ni	5	Ni	5	FeC	Fe+LiF	26	Cd	1
K4	Al	28	CaF ₂	22	Pb	5	Ni	20	Ni	5	FeC	Fe+LiF	24	Cd	1
K6	Al	25	BIF ₃	25	Pb	5	Pb	20	Ni	15	C	Fe+LiF	24	Cd	1
K8	Al	20	CaF ₂	30	Pb	15	Bi	10	Ni	10	C	Fe+LiF	29	B ₄ C	1

The data for verification is processed through the neutron flux distribution in the BSA and the neutron spectrum produced by the BSA. The simulation result

of the distribution of epithermal neutron flux in DLBSA using the PHITS is shown in Figure 10.

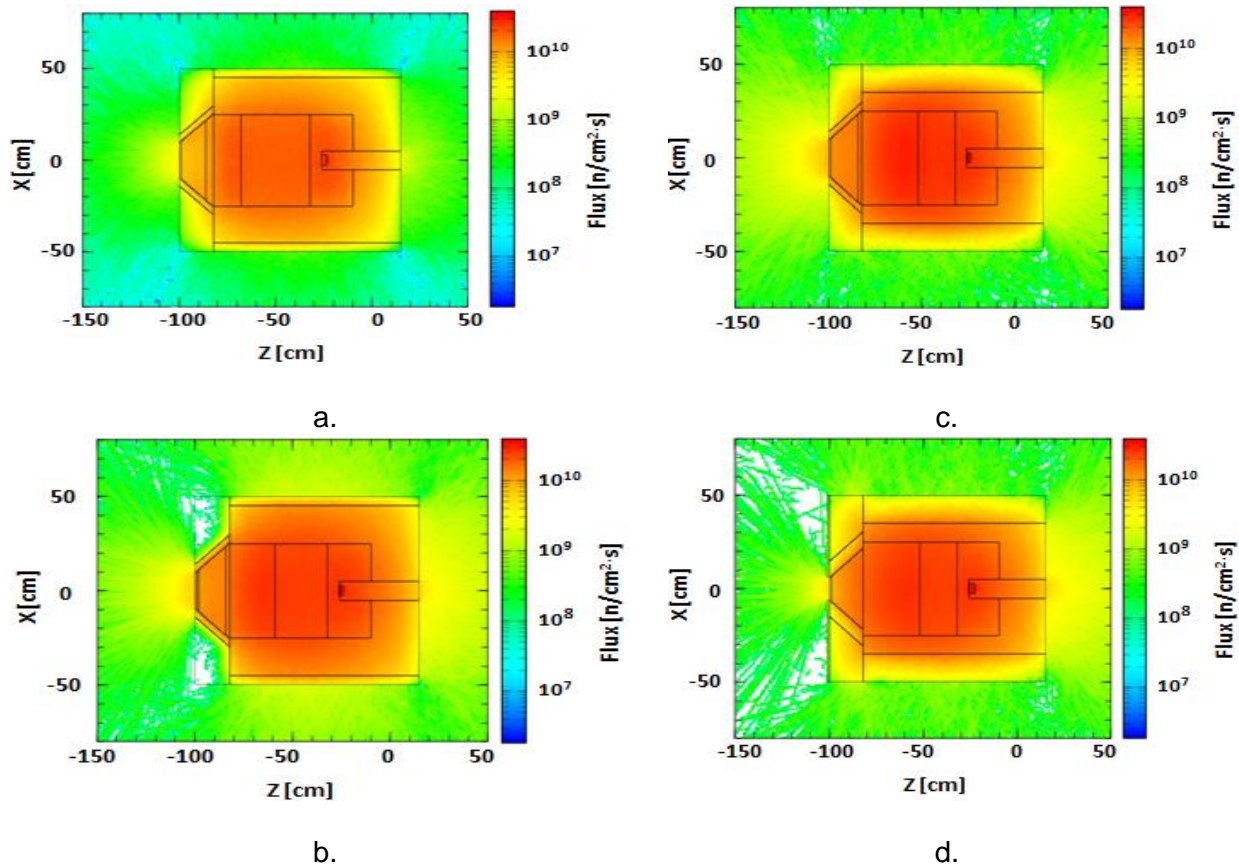


Figure 10 Distribution of epithermal neutron flux in double layer BSA a. K3, b. K4, c.K6, d.K8

The epithermal neutron flux is distributed inside of the double layer BSA. The highest intensity is found in the moderator and decline after passing the collimator and filter. The highest intensity is found in the moderator and decline after passing the collimator and filter. The decrease in the epithermal neutron flux can be attributed to the decrease in the energy of epithermal neutrons, transforming them into thermal neutrons [22]. The value of epithermal neutron flux at the end of the collimator is more than 1.0×10^9 n/cm².s.

The spectrum of neutron beams produced by the DLBSA is shown in Figure 11. Based on the figure, the spectrum demonstrates a narrow peak at 10^{-2} MeV or 10 keV. It suggests that the neutron beams that exit the end of collimator (aperture) are dominantly epithermal neutrons. Such energy of neutron is needed in a BNCT therapy for deeply located cancers [23].

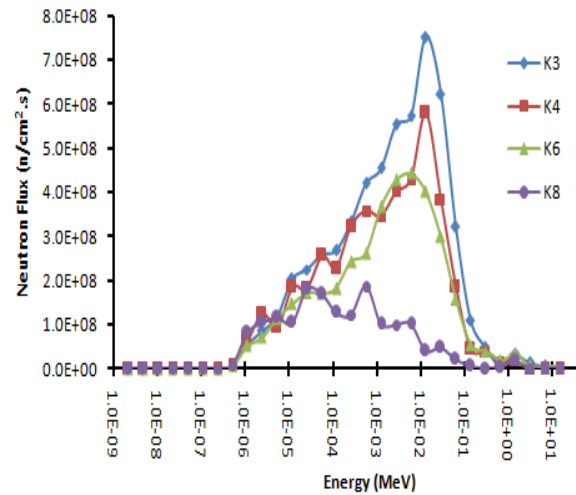


Figure 11 Spectrum of neutron flux produced by DLBSA a. K3, b. K4, c.K6, d.K8

Table 5 Comparison of computed neutron beam parameter using MCNPX and PHITS on DLBSA model optimized by the GA method

K	Code	$\Phi_{\text{epi}} \times 10^9$ (n/cm ² .s)	$\Phi_{\text{epi}}/\Phi_{\text{th}}$	$\Phi_{\text{epi}}/\Phi_{\text{fast}}$	$D_{\text{fast}}/\Phi_{\text{epi}} \times 10^{-13}$ (Gy.cm ²)	$D_{\gamma}/\Phi_{\text{epi}} \times 10^{-13}$ (Gy.cm ²)
3	MCNPX	1.04	231	28	1.98	0.15
	PHITS	2.61	968	22	1.03	0.62
4	MCNPX	1.01	367	53	1.71	0.15
	PHITS	2.54	286	23	0.88	0.86
6	MCNPX	1.29	496	36	1.75	0.12
	PHITS	2.88	931	32	0.67	0.65
8	MCNPX	1.06	431	32	1.34	0.14
	PHITS	2.61	191	22	0.06	0.68
	IAEA	> 1.00	> 100	> 20	< 2.00	< 2.00

Comparison of 5 parameters of neutron beams using the PHITS code is shown in Table 5. The data in Table 5 suggest that the values of neutron beam parameters computed using the PHITS code has successfully met the IAEA standard. The value of epithermal neutron flux computed using the PHITS code is higher than that of MCNPX computation. Such difference may result from the database used by each of the software. The MCNPX uses ENDF/B-VI-6 database, while the PHITS uses JENDL-4.0 database [24]. However, both MCNPX and PHITS results have 0.995 correlations. It suggests that the data have similar patterns.

4.0 CONCLUSION

DLBSA has been successfully optimized using the genetic algorithm method. The optimization is aimed to obtain a maximum solution of DLBSA configuration such that the resulting radiation beams satisfy the requirement for BNCT. The optimization of double-layered BSA using the genetic algorithm method results in four (4) individuals that can produce optimal radiation beams. The most desirable configuration is obtained by combining: (1) Al with either one of CaF₂ or PbF₂ material as moderator, (2) Pb with one of Ni or Pb as reflector, (3) Ni with FeC, or C material as collimator, (4) using FeC+LiF and Cd as the filter for fast and thermal neutron and Pb as gamma filter. The parameters of radiation beams resulted by those four configurations of DLBSA has satisfied the IAEA standard.

The DLBSA model is verified using the PHITS code results in thermal neutron beams having energy of < 10⁻⁶ MeV, epithermal neutrons of 10⁻⁶ - 10⁻² MeV and fast neutrons of > 10⁻² MeV. The resulting spectral curve also suggests that the percentage of epithermal neutron is largest, with energy peak at 10² MeV. It implies that the outgoing neutron beams from the end of the collimator has been dominated by epithermal neutrons. Results from the verification of the four optimal configurations of DLBSA show that the five parameters of the resulting radiation beam meet the IAEA standards.

Acknowledgment

The author expresses his gratitude to LPPM Unsoed, which has fully funded this research through the 2021 Unsoed Basic Research Grant with Contract Number 1068/UN23/HK02/2021.

References

- [1] Yura, Y., Fujita, Y. 2013. Boron Neutron Capture Therapy as a Novel Modality of Radiotherapy for Oral Cancer: Principle and Antitumor Effect. *Oral Science International*. 10(1): 9-14. [http://dx.doi.org/10.1016/S1348-8643\(12\)00046-8](http://dx.doi.org/10.1016/S1348-8643(12)00046-8).
- [2] Sauerwein, W. A. G. 2012. *Neutron Capture Therapy*. New York: Springer.
- [3] Taskaev, S. Y., Kanygin, V. V., Byvaltsev, V. A., Zaboronok, A. A., Volkova, O. Y., Mechetina, L. V., Nakai, K. 2018. Opportunities for using an Accelerator-based Epithermal Neutron Source for Boron Neutron Capture Therapy. *Biomedical Engineering*. 52(2): 73-76. <http://dx.doi.org/10.1007/s10527-018-9785-0>.
- [4] Peng, M., He, G. Z., Zhang, Q. W., Shi, B., Tang, H. Q., Zhou, Z. Y., 2019. Study of Neutron Production and Moderation for Sulfur Neutron Capture Therapy. *Nuclear Science and Techniques*. 30(1): 2. <http://dx.doi.org/10.1007/s41365-018-0529-3>.
- [5] Kreiner, A. J., Bergueiro, J., Cartelli, D., Baldo, M., Castell, W., Asoca, J. G., Mercuri, D. 2016. Present Status of Accelerator-based BNCT. *Reports of Practical Oncology & Radiotherapy*. 21(2): 95-101. <http://dx.doi.org/10.1016/j.rpor.2014.11.004>.
- [6] Kiyonagi, Y. 2018. Accelerator-based Neutron Source for Boron Neutron Capture Therapy. *Therapeutic Radiology and Oncology*. 2. <http://dx.doi.org/10.21037/tro.2018.10.05>.
- [7] Zaidi, L., Kashaeva, E. A., Lezhnin, S. I., Malyshkin, G. N., Samarin, S. I., Sycheva, T. V., Frolov, S. A. 2017. Neutron-beam-shaping Assembly for Boron Neutron-capture Therapy. *Physics of Atomic Nuclei*. 80(1): 60-66. <http://dx.doi.org/10.1134/S106377881701015X>.
- [8] International Atomic Energy Agency. 2001. Current Status of Neutron Capture Therapy, Vienna.
- [9] Tanaka, H., Sakurai, Y., Suzuki, M., Masunaga, S., Mitsumoto, T., Fujita, K., Ono, K. 2011. Experimental Verification of Beam Characteristics for Cyclotron-based Epithermal Neutron Source (C-BENS). *Applied Radiation and Isotopes*. 69(12): 1642-1645. <http://dx.doi.org/10.1016/j.apradiso.2011.03.020>.
- [10] Hashimoto, Y., Hiraga, F., Kiyonagi, Y. 2015. Optimal Moderator Materials at Various Proton Energies Considering Photon Dose Rate After Irradiation for an Accelerator-driven ⁹Be(p,n) Boron Neutron Capture

- Therapy Neutron Source. *Applied Radiation and Isotopes*. 106: 88-91. <http://dx.doi.org/10.1016/j.apradiso.2015.07.027>.
- [11] Khorshidi, A. 2017. Accelerator Driven Neutron Source Design via Beryllium Target and ^{208}Pb Moderator for Boron Neutron Capture Therapy in Alternative Treatment Strategy by Monte Carlo Method. *Journal of Cancer Research and Therapeutics*. 13(3): 456. <http://dx.doi.org/10.4103/0973-1482.179180>.
- [12] Rasouli, F. S., Masoudi S. F. 2012. Design and Optimization of a Beam Shaping Assembly for BNCT based on D-T Neutron Generator and Dose Evaluation using a Simulated Head Phantom. *Applied Radiation and Isotopes*. 70(12): 2755. <http://dx.doi.org/10.1016/j.apradiso.2012.08.008>.
- [13] Fantidis, G. J., Nicolaou, G. 2018. Optimization of Beam Shaping Assembly design for Boron Neutron Capture Therapy based on a Transportable Proton Accelerator. *Alexandria Engineering Journal*. 57: 2333-2342. <http://dx.doi.org/10.1016/j.aej.2017.08.004>.
- [14] Kasesaz, Y., Khalafi, H., Rahmani, F. 2014. Design of an Epithermal Neutron Beam for BNCT in Thermal Column of Tehran Research Reactor. *Annals of Nuclear Energy*. 68: 234-238. <http://dx.doi.org/10.1016/j.anucene.2014.01.014>.
- [15] Hu, G., Hu, H. S., Wang, S., Pan, Z. H., Jia, Q. G., Yan, M. F., Yan, M. F. 2016. The Neutron Channel Design— A Method for Gaining the Desired Neutrons. *AIP Advances*. 6: 1-12. <https://doi.org/10.1063/1.4972203>.
- [16] Turkmen, M., Ergun, S., Colak, U. 2017. A New Method in Beam Shaping: Multi-objective Genetic Algorithm Method Coupled with a Monte Carlo based Reactor Physics Code. *Progress in Nuclear Energy*. 99: 165-176. <https://doi.org/10.1016/j.pnucene.2017.05.008>.
- [17] Rocha, I. B. C. M., Parente Jr, E., Melo, A. M. C. 2014. A Hybrid Shared/distributed Memory Parallel Genetic Algorithm for Optimization of Laminate Composites. *Composite structures*. 107: 288-297. <http://dx.doi.org/10.1016/j.compstruct.2013.07.049>.
- [18] Kim, S. B., & Moon, H. J. 2010. Use of a Genetic Algorithm in the Search for a Near-optimal Shielding Design. *Annals of Nuclear Energy*. 37: 120-129. <https://doi.org/10.1016/j.anucene.2009.11.014>.
- [19] Pelowitz, D. B. 2005. MCNPXTM User's Manual. Los Alamos National Laboratory, Los Alamos. https://www.mcnp.ir/admin/imgs/1354176297.2.6.0_Users_Manual.pdf.
- [20] Sato, T., Niita, K., Matsuda, N., Hashimoto, S., Iwamoto, Y., Noda, S., Okumura, K. 2013. Particle and Heavy Ion Transport Code System PHITS, version 2.52. *Journal of Nuclear Science and Technology*. 50(9): 913-923. <http://dx.doi.org/10.1080/00223131.2013.814553>.
- [21] Aghara, S. K., Sriprisan, S. I., Singleterry, R. C., & Sato, T. 2015. Shielding Evaluation for Solar Particle Events using MCNPX, PHITS and OLTARIS Codes. *Life Sciences in Space Research*. 4: 79-91. <https://doi.org/10.1016/j.lssr.2014.12.003>.
- [22] Shaaban, I., Albarhoum, M. 2015. Design Calculation of an Epithermal Neutronic Beam for BNCT at the Syrian MNSR using the MCNP4C Code. *Progress in Nuclear Energy*. 78: 297-302. <http://dx.doi.org/10.1016/j.pnucene.2014.10.005>.
- [23] Faghihi, F., Khalili, S. 2013. Beam Shaping Assembly of a D-T Neutron Source for BNCT and its Dosimetry Simulation in Deeply-seated Tumor. *Radiation Physics and Chemistry*. 89: 1-13. <https://doi.org/10.1016/j.radphyschem.2013.02.003>.
- [24] Yang, Z. Y., Tsai, P. E., Lee, S. C., Liu, Y. C., Chen, C. C., Sato, T., Sheu, R. J. 2017. Inter-comparison of Dose Distributions Calculated by FLUKA, GEANT4, MCNP, and PHITS for Proton Therapy. *EPJ Web of Conferences*. 153: 04011. EDP Sciences. <http://dx.doi.org/10.1051/epjconf/201715304011>.